IEEE Access
Multidisciplinary ⋮ Rapid Review ⋮ Open Access Journal

Received February 10, 2021, accepted February 24, 2021, date of publication February 26, 2021, date of current version March 9, 2021.

Digital Object Identifier 10.1109/ACCESS.2021.3062627

UAV-Enabled Wireless Backhaul Networks Using Non-Orthogonal Multiple Access

NADIA IRADUKUNDA[1], QUOC-VIET PHAM[2], (Member, IEEE), MING ZENG[3], (Member, IEEE), HEE-CHEOL KIM[4], AND WON-JOO HWANG[5], (Senior Member, IEEE)

[1]Department of Information and Communication System, Inje University, Gimhae 50834, South Korea
[2]Korean Southeast Center for the 4th Industrial Revolution Leader Education, Pusan National University, Busan 46241, South Korea
[3]Department of Electrical Engineering and Computer Engineering, Laval University, Quebec, QC G1V 0A6, Canada
[4]Department of Computer Engineering, Inje University, Gimhae 50834, South Korea
[5]Department of Biomedical Convergence Engineering, Pusan National University, Yangsan 50612, Republic of Korea

Corresponding author: Won-Joo Hwang (wjhwang@pusan.ac.kr)

This work was supported in part by the National Research Foundation of Korea (NRF) Grant funded by the Ministry of Science and Information and Communications Technology (ICT) (MSIT), Korean Government under Grant NRF-2019R1C1C1006143 and Grant NRF-2019R1I1A3A01060518, in part by the Institute of ICT Planning and Evaluation (IITP) Grant funded by the Ministry of Science and ICT (MSIT), Korean Government through the Artificial Intelligence Convergence Research Center, Pusan National University under Grant 2020-0-01450, and in part by the Ministry of Science and ICT (MSIT), South Korea, through the Grand Information Technology Research Center Support Program supervised by the Institute for Information, Communications Technology Planning, and Evaluation (IITP) under Grant IITP-2021-2016-0-00318.

ABSTRACT Owing to their potential mobility and agility, unmanned aerial vehicles (UAVs) have captured predominant interests in sustaining 5G wireless communication and beyond. In this paper, we scrutinize the downlink transmission of UAV-enabled wireless backhaul networks in which non-orthogonal multiple access is incorporated to boost up the massive connectivity and high spectra efficiency. More precisely, our aim is to maximize the worst ground user's achievable rate by optimizing bandwidth allocation, UAV's power allocation and placement. The formulated problem is non-convex and not easy to solve optimally. Consequently, to deal with the complexity and non-convexity of our problem, we develop a path following procedure and generate a less-onerous algorithm that is iteratively run till convergence. The simulation results are executed to validate not only the effectiveness, but also the convergence of the proposed method. In addition, a comparison with other alternative schemes is depicted to divulge the outperformance of our proposed algorithm.

INDEX TERMS Unmanned aerial vehicles (UAVs), wireless backhaul (WB), non-orthogonal multiple access (NOMA), 5G wireless communication and beyond, path following procedure.

I. INTRODUCTION

The up-to-the-minute discoveries consider unmanned aerial vehicles (UAVs) as one of the most propitious paradigms for quenching the ever-ending thirst of ubiquitous connectivity in 5G and beyond [1], [2]. UAVs have the ability to provide a strong line-of-sight (LoS) connection, and a flexible mobility which can be utilized to boost up the communication performance [3]. In addition, UAVs differ from the existing terrestrial infrastructure in the way they are connected to the core network [4]. To achieve a reliable communication for UAVs, the wireless backhaul (WB) emerged as a viable candidate due to its cost-effectiveness and flexibility comparatively to its wired counterpart. Nonetheless, the UAV transmission to the core backhaul network is characterized by heterogeneous links and thus necessitates a high capacity of WB links [1]. Therefore, a lot of attention has been drawn to WB as a limelight in UAVs communication networks [5].

The various topics of WB in UAVs have been explored recently [4]–[7]. More specifically, [4] considered the backhaul for low altitude UAVs. In virtue of stochastic geometry, the authors analyzed the performance of UAVs-based WB in urban environments. In addition, [5] investigated the backhaul-aware robustness by exploring the effect of a variety of WB on the users with respect to their data rates. The WB top rate and the bandwidth of a drone-base station (BS) phenomenally affected the number of served users. Reference [6] examined the optimum value of resource and user

The associate editor coordinating the review of this manuscript and approving it for publication was Walid Al-Hussaibi.

association on a system of multiple UAV-mounted BS with in-band WB.

To boost up the massive connectivity and high spectra efficiency of UAV-enabled networks, non-orthogonal multiple access (NOMA) is of paramount importance [8]–[15]. Unlike other traditional orthogonal multiple access (OMA) techniques, such as TDMA, OFDMA, the basic idea behind NOMA is to serve multiple users via the same orthogonal resource (e.g., time, code, and frequency) by using superposition coding (SC) at the transmitting side and successive interference cancellation (SIC) at the receiving side. Sohail *et al.* in [8] considered a NOMA for UAVs communication and discussed the deployment scenarios of aerial BS, where the issues of coverage and capacity were well tackled. A novel wireless spectrum management strategy was explored in [13] to maximize the efficiency for NOMA-IoT networks. The idea of backscatter communications using NOMA was discussed in [14]. By basing on NOMA designs, a multi-objective joint optimization of resource and power allocation was well addressed in [15] while ensuring the minimum transmit power. There has been a number of works that focused on utilizing NOMA in UAV communication system [16]–[30], [32]. Tan *et al.* [16] computed the ergodic capacity of NOMA-aided systems with a great aim of alleviating the spectrum dearth. In virtue of moment generating function (MGF) technique, and together with stochastic geometry; it was proven that unlike half duplex (HD), higher spectrum efficiency is attainable in NOMA aided full duplex (FD) – HetNets. In addition, the outage probability of FD-NOMA was analyzed in [17] for UAV communications. Moreover, [9] scrutinized the performance of a UAV-enabled systems by computing the outage probability of a network of two ground users (GUs). By comparing NOMA and OMA technologies in the same network topology, it was deduced that NOMA outperformed OMA. In the same way, the idea of Fog UAV was studied in [19] by introducing NOMA scheme. An optimization of energy efficiency was attained by employing a two sided matching technique and a swapping algorithm. By taking into consideration the admission and placement control, [20] presented a low complexity mechanism that improved the quality and the quantity of served users to a maximum level. Placement and power allocation were also jointly optimized in [11] for a NOMA-based UAV systems. By updating the decoding order, [22] maximized the sum rate of NOMA-UAV by optimizing both the power and UAV location. Kilzi *et al.* in [23] analyzed the strategies of placing the UAV in a two-cell NOMA COMP system, so as to sustain a saddled BS. In addition, [25] carried out an optimization task of minimizing the energy consumption in UAV-based multi-edge computing (MEC), with an intention of maintaining the fairness between user equipments (UEs). Zhang *et al.* in [27] aimed at lessening the delay of content delivery by introducing a Q-learning caching technique for NOMA-based UAV's trajectory and spectrum management. The approximation of UAV to UAV links [28] as hotspots with the downlink co-operative NOMA resulted in the reduction of the enormous congestion in LTE and future networks. NOMA was utilized to serve one ground user (GU) and a UAV in [30], where the UAV acted as a DF relay to enlarge the source's scope. Similarly, [31] performed a study on residual impairments that occur at the transceivers of a UAV multi way networks. Jiang *et al.* in [32] purposed to minimize the UAV's consumed power in NOMA networks while taking into consideration the optimum value of both the UAV's transmit power and location. Furthermore, Nasir *et al.* [33] considered UAV-enabled system that serve many GUs by incorporating NOMA scheme.

Motivated by [33], we move forward to explore the WB in UAV-enabled communication, where the WB is considered between a macro-base station (MBS) and a single-antenna UAV-BS. On another front, several works such as [34]–[36] investigated the wireless backhaul in UAV communications, where [34] brought up a novel cooperative NOMA for spatial model of the UAV-assisted WB networks. In virtual of Lipschitz continuity, the maximum sum rate of all users was achieved. In [35], multiple UAVs with multi-hop backhauls were used to support a multitude of GUs so as to maximize the common throughput. With the objective of reducing the UAV's transmit power, [36] investigated the UAV position and resource allocation by accounting backhaul limitation of UAV. In contrast to [34]–[36], we aim at maximizing the worst GU's achievable rate by taking into consideration the WB impact on UAV-enabled communication. In our system, we take into consideration only a single-antenna UAV due to the fact that UAV-enabled downlink communication displays lesser scattering compared to conventional cellular communications, which is different from the multi UAVs work that was performed in [35]. To the best of authors' knowledge, this formulated problem is not available in the open literature. The main contributions of this paper are summarized as follow:

- We first expound our considered system model and problem formulation in Section II, where the MBS communicates with a single-antenna UAV-BS via WB and UAV-BS serves a large number of GUs via wireless access (WA) by incorporating NOMA scheme. We aim at maximizing the GU's worst achievable rate while optimizing the bandwidth allocation so as to steer clear the interference between WB and WA links, the UAV's power allocation and placement so as to ensure a better coverage. For a viable communication, the WB data rate is assumed to be greater than the WA data rate and SIC is taken into consideration since NOMA needs an elaborate user signal detection.
- In order to convert the formulated non-convex objective function into convex approximation series, we develop a path following procedure, which is characterized by a less-onerous and fast convergence for the optimal spectrum, power and placement allocation. The proposed algorithm is discussed in Section III.
- Simulations are executed using numerical examples and they confirm the efficacy and outperformance of the proposed algorithm. The simulation results and conclusions

TABLE 1. Table of abbreviations.

Abbreviations	Definition
UAVs	Unmanned aerial vehicles
5G	Fifth generation
NOMA	Non-orthogonal multiple access
TDMA	Time division multiple access.
OFDMA	Orthogonal frequency division multiple access
WB	Wireless backhaul
WA	Wireless access
LoS	Line of Sight
BS	Base station
MGF	Moment generating function
HD	Half duplex
FD	Full duplex
GUs	Ground users
MEC	Multi-edge computing
UE	User equipment
LTE	Long term evolution
DF	Decode and forward
MBS	Macro base station
SC	Superposition coding
SIC	Successive interference cancellation
CSI	Channel state information
3D	Three dimension

TABLE 2. Table of notations.

Notations	Definitions
N	Number of GUs
n	Near-by user
$i(n), j$	Far user
N_1	Set of near-by GUs
N_2	Set of far GUs
B	System bandwidth
σ	Noise power density
P_n	Transmit power from the UAV to GU n
θ_n	Fraction of WA bandwidth
P	maximum power or power budget of GUs
P_tol	tolerance power
$h_{\max}$	Maximum UAV height
$h_{\min}$	Minimum UAV height
$\rho_{n,m,u}$	2D projection of GUs, MBS, and UAV, respectively
$x_{n,m,u}$	Horizontal coordinate of GUs, MBS, and UAV, respectively
$y_{n,m,u}$	Vertical coordinate of GUs, MBS, and UAV, respectively
g	Channel gain
k	Feasible point
$R_{i(n)}$, R_j	Rate of far GU
R_n	Rate of near-by GU
R_{wb}	Rate of wireless backhaul
K	Iteration number upon convergence
ψ_0	Channel power gain at distance 1 m
ϵ_{tol}	Stopping criterion
C	Cell radius

are drawn in Section IV and Section V, respectively. The tables of abbreviations and notations and their corresponding definitions are provided in Table 1, and Table 2, respectively.

II. SYTEM MODEL AND PROBLEM FORMULATION

The block diagram of the considered UAV-enabled WB networks is depicted in Fig. 1. The network system is comprised of one MBS, one single-antenna rotary-wing UAV, and N GUs. We put into consideration the downlink layer, where the MBS communicates with UAV via WB which is assigned α_1 as allocated bandwidth partition factor, and UAV serves a large number of GU via WA links by employing NOMA. The WA links are assigned α_2 as allocated bandwidth partition factor. For simplicity of our analysis, we consider no direct communication between MBS and N GUs due to some geographical obstacles [34]. Here, N GUs are only served by UAV by assuming that UAV possesses the channel state information (CSI) of all the GUs. We suppose that N GUs are divided into two sets. We have set a half of GUs, i.e., from 1 to $N/2$ to be located to the cell center; thus considered as near-by GUs. On the other hand, the latter half of GUs, i.e., from $N/2+1$ to N are to be located at the cell edge; and thus referred as far GUs [33]. More importantly, it is worth noting that the half GUs which occupy the cell center are randomly distributed there, and the same analogy is being applied to the far GUs which are randomly distributed at the cell edge. The set of GUs, near-by GUs, and far GUs are denoted by $\mathcal{N} = \{1, \ldots, N\}$, $\mathcal{N}_1 = \{1, \ldots, N/2\}$ and $\mathcal{N}_2 = \{N/2+1, \ldots, N\}$, respectively.

The 3D location of the UAV, MBS, and GU n are denoted by (x_u, y_u, h), $(x_m, y_m, 0)$, and $(x_n, y_n, 0)$ respectively. By projecting these 3D locations on the horizontal plane, UAV, MBS and users can be denoted by $\boldsymbol{\rho}_u = (x_u, y_u)$, $\boldsymbol{\rho}_m = (x_m, y_m)$, $\boldsymbol{\rho}_n = (x_n, y_n)$; respectively. Since the UAV has the ability to enable strong LoS communication links [10], [37], the free space channel model can appropriately estimate the air to ground channel [10], [32]. Thus, the channel power gain between UAV to GU n is calculated as

$$g_n = \psi_0 d_n^{-2},$$

where ψ_0 is the channel power gain at the reference distance $d_0 = 1$ m and $d_n = \sqrt{h^2 + \|\boldsymbol{\rho}_u - \boldsymbol{\rho}_n\|^2}$. In other words,

$$d_n = \sqrt{h^2 + (\boldsymbol{x}_u - \boldsymbol{x}_n)^2 + (\boldsymbol{y}_u - \boldsymbol{y}_n)^2}.$$

Similarly, the channel power gain between the MBS and UAV is modeled as

$$g_m = \psi_0 d_m^{-2},$$

with $d_m = \sqrt{h^2 + |\boldsymbol{\rho}_u - \boldsymbol{\rho}_m\|^2}$, which can be re-written as

$$d_m = \sqrt{h^2 + (\boldsymbol{x}_u - \boldsymbol{x}_m)^2 + (\boldsymbol{y}_u - \boldsymbol{y}_m)^2}.$$

The UAV engages NOMA to pair each near-by GU n with one of the far users $i(n) = n + N/2$ to share the same resource block, thus creating a cluster, say cluster n. More specifically,

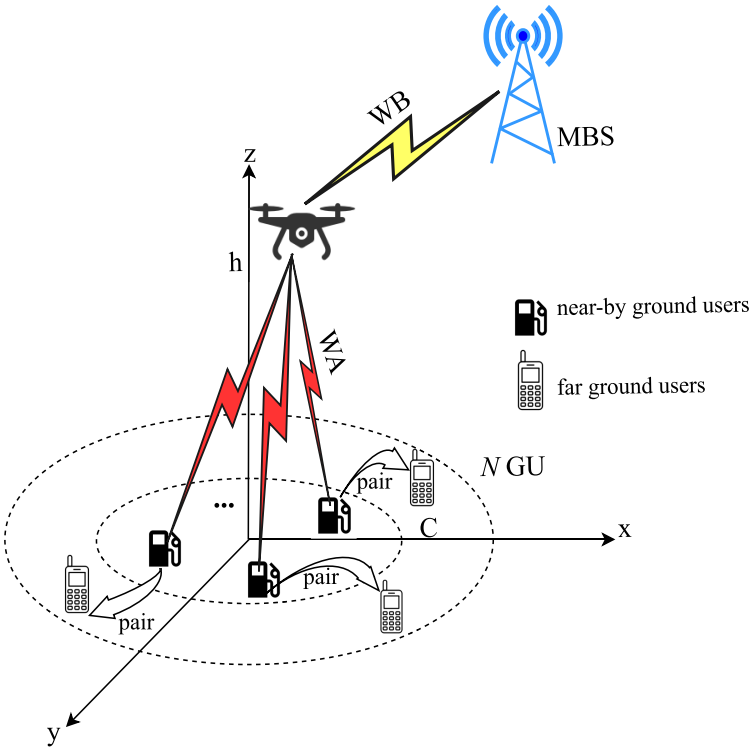

FIGURE 1. An exemplary scenario of UAV-enabled WB networks using NOMA.

the pairing strategy between near GU and far GU is mainly based on the minimum Euclidean distance [33].[1]

Note that near-by GU n applies SIC before decoding its signal in order to cancel the interference from the far GU. Therefore, the achievable rate of a near-by GU in nats/sec/Hz is given as

$$R_n = \theta_n \ln\left(1 + p_n g_n / n_0 \theta_n\right),$$

where $n_0 = \sigma^2 B$ with σ^2 being the noise power density, and B being the system bandwidth, p_n is the transmit power from the UAV to GU n, and θ_n is the fraction of WA bandwidth allocated to cluster n such that $\sum_{n=1}^{N/2} \theta_n = \alpha_2$. Since the far GU in NOMA does not execute SIC prior to the decoding of its signal, the achievable rate of a far GU is given by

$$R_{i(n)} = \theta_n \ln\left(1 + \frac{p_{i(n)} g_{i(n)}}{n_0 \theta_n + p_n g_{i(n)}}\right).$$

For the WB link, the transmission rate can be written as

$$R_{wb} = \alpha_1 \ln\left(1 + p_m g_m / \alpha_1 n_0\right),$$

where p_m is the transmit power of the MBS.

In this paper, our objective is to maximize the worst GU's achievable rate by optimizing the bandwidth allocation, UAV's power allocation and placement. The optimization problem can be formulated as follows:

$$\max \min_{n \in \mathcal{N}} R_n^{\text{NOMA}}(\boldsymbol{\alpha}, \boldsymbol{p}, \boldsymbol{\delta}) \tag{1a}$$
$$\text{s.t. } \alpha_1 + \alpha_2 = 1, \ \boldsymbol{\alpha} > 0 \tag{1b}$$
$$\sum_{n=1}^{N/2} \theta_n = \alpha_2, \theta_n \geq 0, \forall n \in \mathcal{N}_1, \tag{1c}$$
$$p_n \geq 0 \ \forall n, \ \sum_{n=1}^{N} p_n \leq P, \tag{1d}$$
$$x_u^2 + y_u^2 \leq C^2, \tag{1e}$$
$$h_{\min} \leq h \leq h_{\max}, \tag{1f}$$
$$\sum_{n=1}^{N/2} (R_n + R_{i(n)}) \leq R_{wb}, \tag{1g}$$
$$p_{i(n)} \bar{g}_n - p_n \bar{g}_n \geq P_{tol}. \tag{1h}$$

In problem (1), we define $\boldsymbol{\alpha} = \{\alpha_1, \theta_1, \ldots, \theta_{N/2}\}$, $p = \{p_1, \ldots, p_N\}$, $\boldsymbol{\delta} = \{x_u, y_u, h\}$,

$$R_n^{\text{NOMA}}(\boldsymbol{\alpha}, \boldsymbol{p}, \boldsymbol{\delta}) = \begin{cases} R_n, & n \in \mathcal{N}_1, \\ R_{i(n)}, & i(n) \in \mathcal{N}_2, \end{cases} \tag{2}$$

and $\bar{g}_n = \frac{g_n}{n_0}$ as the normalized channel gain.

The constraints (1b) and (1c) are to adjust the feasible sets of bandwidth allocation. The constraint (1d) is for limiting the transmit power allocated to N GUs to a value P. (1e) is for placing the UAV within a circular disc of radius C, whereas (1f) is for fixing the range of UAV's altitude to a value between the minimum and maximum UAV's altitude, $h_{\min}$ and $h_{\max}$. The constraint (1g) is for keeping the total

[1]The process of finding the optimum strategy of pairing and extra complicated user-pairing strategies [38], [39] are beyond the scope of this paper and set aside for our future works. Furthermore, even if the extra aforementioned methods have not been taken into consideration, the performance results are still promising.

transmission rate of the WA links lower than the transmission rate of the WB link. Due to conservation of flow constraint, the outgoing flows from UAV to N GUs shouldn't exceed the incoming flow from MBS to UAV. Therefore, the capacity of WB link plays a predominant role for the transmission to occur. Lastly, (1h) is for limiting the minimum power difference needed to differentiate the signal to be decoded and the remaining uncoded one to a value greater or equal to P_{tol} so as to ensure efficient SIC [12].

It is worth noting that due to the presence of quadratic terms employed by the LoS channel gains, we prefer to introduce these two auxiliary slack vectors, namely $\boldsymbol{\lambda} = \{\lambda_t\}_{t\in\mathcal{N}\cup\{m\}}$ and $\boldsymbol{\zeta} = \{\zeta_n\}_{n\in\mathcal{N}}$ in (1) so as to make it more tractable.

Therefore, the problem (1) can be re-written as follows:

$$\max \min_{n\in\mathcal{N}} R_n^{\text{NOMA}}(\boldsymbol{\alpha}, \boldsymbol{p}, \boldsymbol{\delta}, \boldsymbol{\lambda}, \boldsymbol{\zeta}) \tag{3a}$$

$$\text{s.t. (1b), (1c), (1d), (1e), (1f), (1h),} \tag{3b}$$

$$\sum\nolimits_{n=1}^{N/2} \theta_n \left(\ln\left(1 + \frac{p_n\psi_0}{n_0\theta_n\zeta_n}\right) + \ln\left(1 + \frac{p_{i(n)}\psi_0}{n_0\theta_n\zeta_{i(n)} + \psi_0 p_n}\right)\right) \leq R_{wb} \tag{3c}$$

$$\lambda_t \geq h^2 + \|\boldsymbol{\rho}_u - \boldsymbol{\rho}_t\|^2, \forall t \in \mathcal{N}\cup\{m\}, \tag{3d}$$

$$\zeta_n \leq h^2 + \|\boldsymbol{\rho}_u - \boldsymbol{\rho}_n\|^2, \forall n \in \mathcal{N}, \tag{3e}$$

$$\zeta_n \geq h^2, \forall n \in \mathcal{N}, \tag{3f}$$

where $R_{wb} = \alpha_1 \ln(1 + p_m\psi_0/\alpha_1 n_0\lambda_m)$, and

$$R_n^{\text{NOMA}}(\boldsymbol{\alpha}, \boldsymbol{p}, \boldsymbol{\delta}, \boldsymbol{\lambda}, \boldsymbol{\zeta}) = \begin{cases} R_n = \theta_n \ln(1 + p_n\psi_0/n_0\theta_n\lambda_n), & n \in \mathcal{N}_1, \\ R_{i(n)} = \theta_n \ln\left(1 + \frac{p_{i(n)}\psi_0}{n_0\theta_n\lambda_{i(n)} + \psi_0 p_n}\right), & i(n) \in \mathcal{N}_2. \end{cases} \tag{4}$$

It is noteworthy that for (3) to be held feasible, the objective function can be enhanced by decreasing $\{\lambda_n\}_{n\in\mathcal{N}}$ and the constraint (3c) can be improved by increasing $\{\zeta_n\}_{n\in\mathcal{N}}$ and/or decreasing λ_m. Despite of that, it is still quite challenging to solve (3) due to its non-convexity. As a result, we apply the inner convex approximation-based path-following algorithm to (3) as detailed below.

III. PROPOSED ALGORITHM

It is obviously noticeable from (3) that the objective function (3a) is a non-concave function and its constraints (1h), (3c),and (3e) are non-convex; which make the problem so onerous to solve optimally [40]. To cope with this difficulty, we introduce the path-following computation by developing the following lemmas.

Lemma 1: Assume $x > 0, y > 0, \theta > 0, \bar{x} > 0, \bar{y} > 0$ and $\bar{\theta} > 0$, for a convex function $f(x, y, \theta) \triangleq \ln(1 + 1/xy)^\theta$ [41],

$$\theta \ln\left(1 + \frac{1}{xy}\right) \geq 2\bar{\theta}\ln\left(1 + \frac{1}{\bar{x}\bar{y}}\right) + \frac{\bar{\theta}(2 - x/\bar{x} - y/\bar{y})}{1 + \bar{x}\bar{y}} - \frac{\bar{\theta}^2 \ln(1 + 1/\bar{x}\bar{y})}{\theta}. \tag{5}$$

Lemma 2: For all $0 \leq x \leq N$ and $\mu \geq \ln(1 + N) + 0.5$,

$$\frac{-\ln(1+x)}{t} \geq 2\frac{\mu - \ln(1+\bar{x})}{\bar{t}} + \frac{\bar{x}}{\bar{t}(1+\bar{x})} - \frac{x}{\bar{t}(1+\bar{x})} - \frac{\mu - \ln(1+\bar{x})}{\bar{t}^2}t - \frac{\mu}{t}.$$

Thus,

$$\frac{\ln(1+x)}{t} \leq -2\frac{\mu - \ln(1+\bar{x})}{\bar{t}} - \frac{\bar{x}}{\bar{t}(1+\bar{x})} + \frac{x}{\bar{t}(1+\bar{x})} + \frac{\mu - \ln(1+\bar{x})}{\bar{t}^2}t + \frac{\mu}{t}. \tag{6}$$

Let $(\boldsymbol{\theta}^{(k)}, \boldsymbol{p}^{(k)}, \boldsymbol{\lambda}^{(k)})$ be a feasible point for problem (3) that is found at $(k-1)$-th iteration. Regarding the function R_n in (3a), using the inequality (5) for $\theta = \theta_n$, $x = n_0/p_n\psi_0$, $y = \theta_n\lambda_n$, $\bar{\theta} = \theta_n^{(k)}$, $\bar{x} = n_0/p_n^{(k)}\psi_0$ and $\bar{y} = \theta_n^{(k)}\lambda_n^{(k)}$ gives out $R_n(\boldsymbol{\theta}, \boldsymbol{p}, \boldsymbol{\lambda}) \geq R_n^{(k)}(\boldsymbol{\theta}, \boldsymbol{p}, \boldsymbol{\lambda})$, where

$$R_n^{(k)}(\boldsymbol{\theta}, \boldsymbol{p}, \boldsymbol{\lambda}) = \tau_n^{(k)} + \beta_n^{(k)}\left(2 - \frac{p_n^{(k)}}{p_n} - \frac{\theta_n\lambda_n}{\theta_n^{(k)}\lambda_n^{(k)}}\right) - \frac{\gamma_n^{(k)}}{\theta_n}, \tag{7}$$

which is a concave function for $0 < \tau_n^{(k)} = 2\bar{\theta}\ln(1 + 1/\bar{x}\bar{y})$, $0 < \beta_n^{(k)} = \bar{\theta}/1 + \bar{x}\bar{y}$ and $0 < \gamma_n^{(k)} = \bar{\theta}^2\ln(1 + 1/\bar{x}\bar{y})$.

Similarly, with regard to the function $R_{i(n)}$, by letting $i(n) = j$, $R_{i(n)}$ become R_j and by applying (5) for $\theta = \theta_n$, $x = 1/p_j\psi_0$, $y = n_0\theta_n\lambda_j + p_n\psi_0$, $\bar{\theta} = \theta_n^{(k)}$, $\bar{x} = 1/p_j^{(k)}\psi_0$ and $\bar{y} = n_0\theta_n^{(k)}\lambda_j^{(k)} + p_n^{(k)}\psi_0$ yields $R_j(\boldsymbol{\theta}, \boldsymbol{p}, \boldsymbol{\lambda}) \geq R_j^{(k)}(\boldsymbol{\theta}, \boldsymbol{p}, \boldsymbol{\lambda})$, where $R_j^{(k)}(\boldsymbol{\theta}, \boldsymbol{p}, \boldsymbol{\lambda}) =$

$$\tau_j^{(k)} + \beta_j^{(k)}\left(2 - \frac{p_j^{(k)}}{p_j} - \frac{n_0\theta_n\lambda_j + p_n\psi_0}{n_0\theta_n^{(k)}\lambda_j^{(k)} + p_n^{(k)}\psi_0}\right) - \frac{\gamma_j^{(k)}}{\theta_n}, \tag{8}$$

which is a concave function for $0 < \tau_j^{(k)} = 2\bar{\theta}\ln(1 + 1/\bar{x}\bar{y})$, $0 < \beta_j^{(k)} = \bar{\theta}/1 + \bar{x}\bar{y}$ and $0 < \gamma_j^{(k)} = \bar{\theta}^2\ln(1 + 1/\bar{x}\bar{y})$.

Then, the lower bounding concave function for (3a) is reformulated as follows:

$$R_n^{\text{NOMA},(k)}(\boldsymbol{\theta}, \boldsymbol{p}, \boldsymbol{\lambda}) = \begin{cases} R_n^{(k)}(\boldsymbol{\theta}, \boldsymbol{p}, \boldsymbol{\lambda}), & n \in \{1, \ldots, N/2\}, \\ R_j^{(k)}(\boldsymbol{\theta}, \boldsymbol{p}, \boldsymbol{\lambda}), & j \in \{N/2 + 1, \ldots, N\}, \end{cases} \tag{9}$$

with $R_n^{(k)}$, and $R_j^{(k)}$ being computed in (7), and (8), respectively.

Next, to handle the non-convexity of (3c), we firstly re-write it as $\sum_{n=1}^{N/2} R_n + \sum_{n=N/2+1}^{N} R_{i(n)} \leq R_{wb}$. Regarding (3c)'s left-hand side, we apply inequality (6) to both R_n and R_j respectively. Note that $j = i(n)$ as mentioned before. So by applying (6) to R_n, for $1/t = \theta_n$, $x = p_n\psi_0/n_0\theta_n\zeta_n$, $1/\bar{t} = \theta_n^{(k)}$, $\bar{x} = p_n^{(k)}\psi_0/n_0\theta_n^{(k)}\zeta_n^{(k)}$, we get $R_n(\boldsymbol{\theta}, \boldsymbol{p}, \boldsymbol{\zeta}) \leq \bar{R}_n^{(k)}(\boldsymbol{\theta}, \boldsymbol{p}, \boldsymbol{\zeta})$, where

$$\bar{R}_n^{(k)}(\boldsymbol{\theta}, \boldsymbol{p}, \boldsymbol{\zeta}) = \hat{\tau}_n^{(k)} + \hat{\beta}_n^{(k)}\frac{p_n\psi_0}{n_0\theta_n\zeta_n} + \frac{\hat{\gamma}_n^{(k)}}{\theta_n} + \mu\theta_n, \tag{10}$$

for $\hat{\tau}_n^{(k)} = -2(\mu - \ln(1 + \bar{x}))/\bar{t} - \bar{x}/\bar{t}(1 + \bar{x})$, $\hat{\beta}_n^{(k)} = 1/\bar{t}(1 + \bar{x})$ and $\hat{\gamma}_n^{(k)} = (\mu - \ln(1 + \bar{x}))/\bar{t}^2$.

From (10), it remains to deal with

$$\frac{p_n\psi_0}{n_0\theta_n\zeta_n} = \frac{\psi_0}{4n_0}\left(\left(p_n+\frac{1}{\theta_n\zeta_n}\right)^2-\left(p_n-\frac{1}{\theta_n\zeta_n}\right)^2\right) \leq \frac{\psi_0}{4n_0}\left(p_n+\frac{1}{\theta_n\zeta_n}\right)^2 = b_n^{(k)}(\theta_n,p_n,\zeta_n) \quad (11)$$

Therefore,

$$\bar{R}_n^{(k)}(\boldsymbol{\theta},\boldsymbol{p},\boldsymbol{\zeta}) = \hat{\tau}_{n^{(k)}} + \hat{\beta}_n^{(k)} b_n^{(k)}(\theta_n,p_n,\zeta_n) + \frac{\hat{\gamma}_n^{(k)}}{\theta_n} + \mu\theta_n, \quad (12)$$

which is a convex function in $(\boldsymbol{\theta},\boldsymbol{p},\boldsymbol{\zeta})$. Next, by applying inequality (6) to R_j for $1/t=\theta_n$, $x=p_j\psi_0/(n_0\theta_n\zeta_j+\psi_0 p_n)$, $1/\bar{t}=\theta_n^{(k)}$, $\bar{x}=p_j^{(k)}\psi_0/(n_0\theta_n^{(k)}\zeta_j^{(k)}+\psi_0 p_n^{(k)})$, we obtain $R_j(\boldsymbol{\theta},\boldsymbol{p},\boldsymbol{\zeta}) \leq \bar{R}_j^{(k)}(\boldsymbol{\theta},\boldsymbol{p},\boldsymbol{\zeta})$, where

$$\bar{R}_j^{(k)}(\boldsymbol{\theta},\boldsymbol{p},\boldsymbol{\zeta}) = \hat{\tau}_j^{(k)} + \hat{\beta}_j^{(k)}\left(\frac{p_j\psi_0}{n_0\theta_n\zeta_j+\psi_0 p_n}\right) + \frac{\hat{\gamma}_j^{(k)}}{\theta_n} + \mu\theta_n, \quad (13)$$

for $\hat{\tau}_j^{(k)} = -2(\mu-\ln(1+\bar{x}))/\bar{t}-\bar{x}/\bar{t}(1+\bar{x})$, $\hat{\beta}_j^{(k)} = 1/\bar{t}(1+\bar{x})$ and $\hat{\gamma}_j^{(k)} = (\mu-\ln(1+\bar{x}))/\bar{t}^2$.

From (13), it remains to cope with

$$\frac{p_j\psi_0}{n_0\theta_n\zeta_j+\psi_0 p_n} = \frac{\frac{\psi_0}{4n_0}\left(\left(p_j+\frac{1}{\theta_n\zeta_j}\right)^2-\left(p_j-\frac{1}{\theta_n\zeta_j}\right)^2\right)}{1+\frac{\psi_0}{4n_0}\left(\left(p_n+\frac{1}{\theta_n\zeta_j}\right)^2-\left(p_n-\frac{1}{\theta_n\zeta_j}\right)^2\right)} \leq \frac{\frac{\psi_0}{4n_0}\left(p_j+\frac{1}{\theta_n\zeta_j}\right)^2}{1+\frac{\psi_0}{4n_0}\left(p_n+\frac{1}{\theta_n\zeta_j}\right)^2} = b_j^{(k)}(\theta_n,p_j,\zeta_j,p_n) \quad (14)$$

Therefore,

$$\bar{R}_j^{(k)}(\boldsymbol{\theta},\boldsymbol{p},\boldsymbol{\zeta}) = \hat{\tau}_j^{(k)} + \hat{\beta}_j^{(k)} b_j^{(k)}(\theta_n,p_j,\zeta_j,p_n) + \frac{\hat{\gamma}_j^{(k)}}{\theta_n} + \mu\theta_n, \quad (15)$$

which is a convex function in $(\boldsymbol{\theta},\boldsymbol{p},\boldsymbol{\zeta})$. Regarding the right-hand side of (3c), by using the first order optimality condition [40] for the function R_{wb}, we get $R_{wb}(\lambda_m) \geq \underline{R}_{wb}^{(k)}(\lambda_m) = R_{wb}(\lambda_m^{(k)}) + \nabla R_{wb}(\lambda_m^{(k)})(\lambda_m-\lambda_m^{(k)})$, where $\nabla R_{wb}(\lambda_m^{(k)}) = \frac{-\alpha_1 p_m\psi_m}{\lambda_m^{(k)}(\lambda_m^{(k)}+p_m\psi_m)}$ and $\psi_m = \frac{\psi_0}{\alpha_1 n_0}$. As a result (3c) can be approximated by the following convex constraint:

$$\sum_{n=1}^{N/2}\bar{R}_n^{(k)} + \sum_{j=\frac{N}{2}+1}^{N}\bar{R}_j^{(k)} \leq \underline{R}_{wb}^{(k)}(\lambda_m). \quad (16)$$

Moreover, to get to grips with the non-convexity of (3e), we consider $f(a)=a^2$ to be convex with respect to a, thus $a^2 \geq 2aa^{(k)} - (z^{(k)})^2$. By applying the same analogy to the constraint (3e), we obtain

$$h^2 + \|\boldsymbol{\rho}_u-\boldsymbol{\rho}_n\|^2 \geq f_n^{(k)}(\boldsymbol{\delta}) = 2hh^{(k)} - (h^{(k)})^2 + 2x_u x_u^{(k)} - (x_u^{(k)})^2 - 2x_u x_n + x_n^2 + 2y_u y_u^{(k)} - (y_u^{(k)})^2 - 2y_u y_n + y_n^2, \quad (17)$$

Consequently (3e) can be rewritten as

$$\zeta_n \leq f_n^{(k)}(\boldsymbol{\delta}), \forall n \in \mathcal{N}. \quad (18)$$

Finally, the constraint on efficient SIC operation (1h) is equivalently transformed as:

$$p_{i(n)} - p_n - \frac{P_{tol}}{\bar{g}_n} \geq 0, \quad (19)$$

and by expressing $\bar{g}_n$ in terms of λ_n, (19) can be rewritten as

$$p_{i(n)} - p_n - \frac{P_{tol}\lambda_n n_0}{\psi_0} \geq 0, \quad (20)$$

which is a convex function.

In short, at the k-th iteration, we solve the following convex optimization problem

$$\max \min_{n\in N} R_n^{\mathrm{NOMA},(k)}(\boldsymbol{\theta},\boldsymbol{p},\boldsymbol{\delta},\boldsymbol{\lambda},\boldsymbol{\zeta}) \quad \text{s.t. (1b), (1c), (1d), (1e), (1f), (3d), (3f), (16), (18), (20).} \quad (21)$$

so as to yield the next iterative feasible point at $(k+1)$ for our formulated problem. This path following iterative process can be repeated till convergence.

Proof: (21) is a convex optimization problem because of the following reasons:

- (1b), (1c), (1d), (1e), (1f),(3d),(3f), are convex and their feasible regions are convex.
- (16) is convex since it is resulted from (3c) that has been convexified using both Lemma 2 with inequality (6) and first optimal condition [40].
- (18) is convex after being quadratically transformed.
- (20) is equivalently convex.

Basing on the aforementioned reasons, (21) maximizes a concave function upon a convex set, and is consequently a convex optimization problem. □

The computation complexity of (21) is $\mathcal{O}(K(5N)^2(11N)^{2.5}+(11N)^{3.5})$, since it implies $5N$ decision variables, and $11N$ linear and quadratic constraints [20], [41]. K denotes the iteration number upon convergence [20], [41]. The steps required to solve our problem are outlined in Algorithm 1. The algorithm stops when the relative difference between objective values of two consecutive iterations is less than a tolerance threshold ϵ_{tol}.

IV. SIMULATION RESULT

In this section, simulation results are executed to divulge the efficacy of our proposed path-following algorithm for UAV-enabled WB. The network topology that is used in the simulations is depicted on Fig. 2. In our simulation settings, $N=30$ users and are randomly distributed within a circular cell of radius $C=300$ m. The near-by GUs are located at the cell center in the area of radius $C/2$, whereas the far GUs are located at the cell edge in the area of radius

Algorithm 1 A Joint Bandwidth Allocation, Power Allocation and Placement Algorithm for a UAV-Enabled WB

1: **Initialization:** Set $k := 0$ and find the initial feasible point $(\boldsymbol{\theta}^{(0)}, \boldsymbol{p}^{(0)}, \boldsymbol{\delta}^{(0)}, \boldsymbol{\lambda}^{(0)}, \boldsymbol{\zeta}^{(0)})$ for the constraints of (3).
2: **repeat**
3: Solve the convex optimization problem (21) in order to get the optimal solution $(\boldsymbol{\theta}^{(k+1)}, \boldsymbol{p}^{(k+1)}, \boldsymbol{\delta}^{(k+1)}\boldsymbol{\lambda}^{(k+1)}, \boldsymbol{\zeta}^{(k+1)})$.
4: Set $k := k + 1$.
5: **until** $\frac{|\Phi^{(k+1)} - \Phi^{(k)}|}{\Phi^{(k)}} \leq \epsilon_{tol}$, where $\Phi^{(k+1)}$ is the value of objective function in (21).

TABLE 3. Simulation parameters.

Parameters	Values
Number of GUs (N)	30
Cell radius (C)	300 m
$h_{\min}$	60 m
$h_{\max}$	600 m
P_m	9 dBm
ρ_m	(700 m, 700 m)
P	6 dBm
P_{tol}	3 dBm
ψ_0	3.24×10^{-4}
σ^2	-174 dBm/Hz
ϵ_{tol}	10^{-4}
Bandwidth (B)	10 MHz

greater than $C/2$ and not beyond C, thus considered as an annulus. Unless otherwise mentioned, the UAV minimum and maximum altitude are set to $h_{\min} = 60$ m and $h_{\max} = 600$ m, respectively. The MBS transmit power and position are set to $P_m = 9$ dBm and $\rho_m = (700, 700)$ m respectively. The limiting power is $P = 6$ dBm, the tolerance power is $P_{tol} = 3$ dBm, the channel power gain at reference distance of $d_0 = 1$ m is $\psi_0 = 3.24 \times 10^{-4}$ that leads to a path loss of 1.42×10^{-4}, the noise power density is $\sigma^2 = -174$ dBm/Hz, the stopping criterion $\epsilon_{tol} = 10^{-4}$, and the system bandwidth is $B = 10$ MHz. The main simulation settings are briefly described in Table 3. By using Matlab and its widely known software for disciplined convex programming, i.e., CVX; our simulations are carried out.

For the sake of proving the outperformance of our work, we compare our proposed algorithm that jointly optimize bandwidth allocation, power allocation and placement (labeled as **BAPAP**), with the 3 other cases namely:

- Bandwidth allocation and power allocation (labelled as **BAPA**): where a joint bandwidth allocation and power allocation is performed with a random placement of UAV.
- Bandwidth allocation and placement (labelled as **BAP**): where the optimization of bandwidth and placement is evaluated with equal power allocation. i.e., $p_n = P/N$.
- Power allocation and placement (labelled as **PAP**): where a joint power allocation and placement with bandwidth allocation factor set as 0.4.

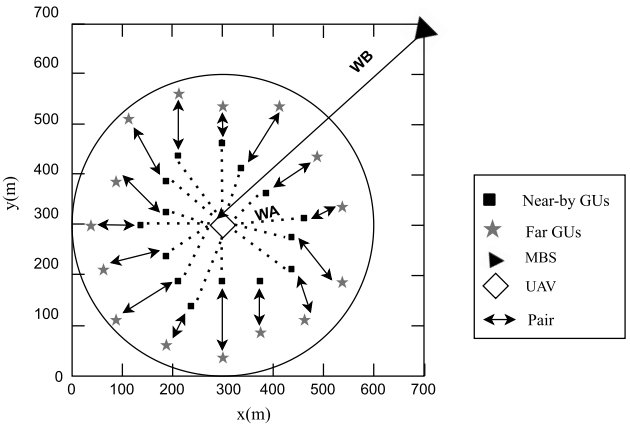

FIGURE 2. Network topology.

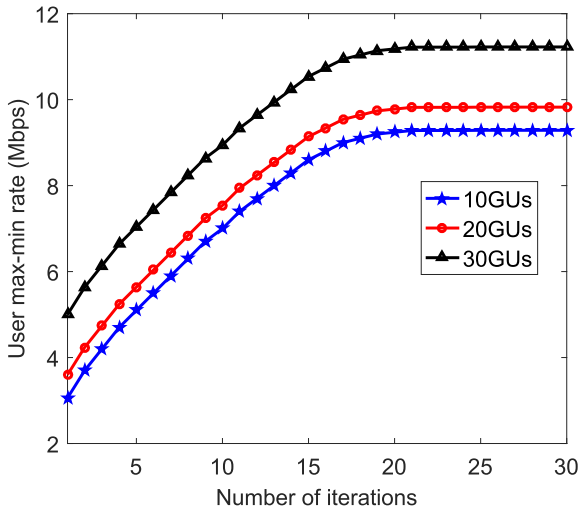

FIGURE 3. Convergence behaviour of the proposed algorithm.

Firstly, we investigate the convergence of our proposed algorithm on Fig. 3 by altering the number of users. As can been seen from the figure, the user max-min rate keeps increasing for about 30 iterations. This reveals that our proposed algorithm takes a fair time in order to converge. Furthermore, we can also deduce that the more the number of users increase, the more the max-min rate decrease. This is due to the fact that when users get increased, the spectrum allocated to each pair of users gets decreased. As a result, the max-min rate of users diminishes with respect to the increase in number of GUs.

Secondly, we evaluate the user max-min rate by altering the MBS transmit power as depicted on Fig. 4. It is accurately deduced that the increase in MBS transmit power leads to an increase in use max-min rate. This is because the more the MBS transmit power goes higher, the more the WB capacity will be. This significantly increases the user rate due to the wireless backhaul's flow conservation constraint. By comparing our proposed BAPAP algorithm with the three aforementioned schemes, it is remarkably seen that BAPAP outperforms them. Intuitively, this outperformance

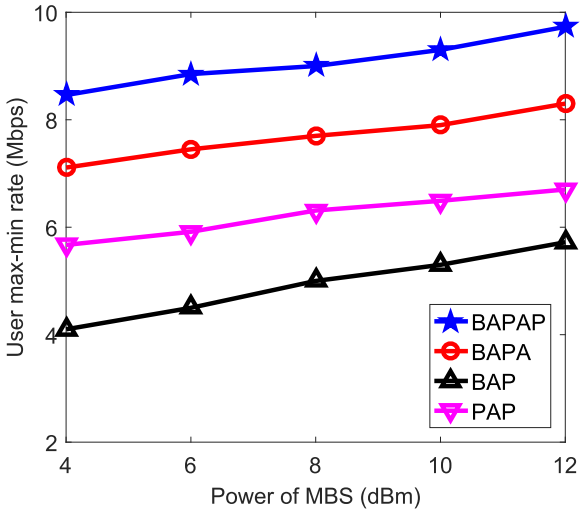

FIGURE 4. User max-min rate vs. power of MBS.

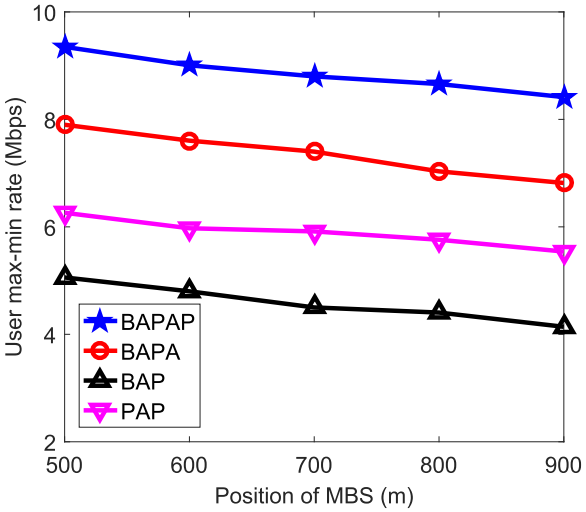

FIGURE 5. User max-min rate vs. position of MBS.

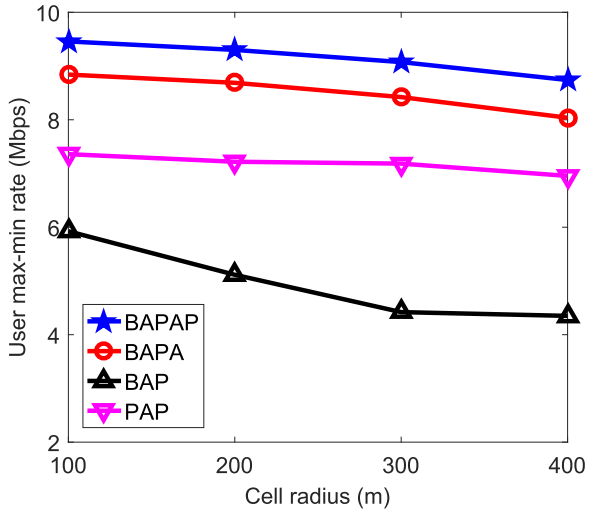

FIGURE 6. User max-min rate vs. cell radius.

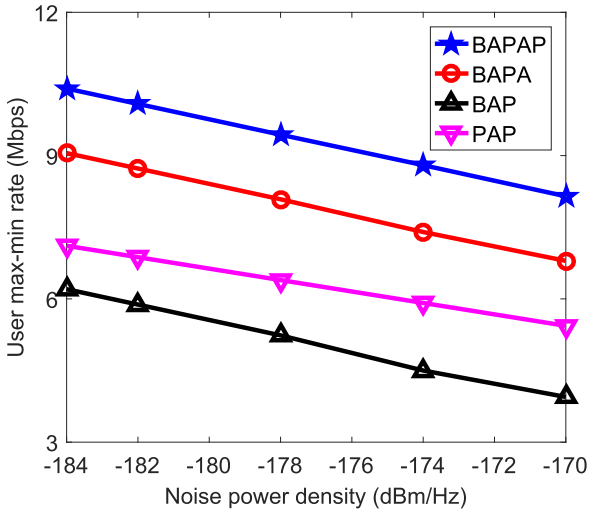

FIGURE 7. User max-min rate vs. noise power density.

is attributed to the fact that our proposed scheme jointly optimizes bandwidth, UAV's power and placement, which seems to be more promising comparatively to BAPA, BAP, PAP that separately optimize one or few parameters in the system. In addition, we can also realize that among all schemes, assuming equal power allocation (BAP) leads to a poor performance system. This shows that an absolute power allocation is predominant for NOMA systems.

Moreover, we scrutinize the user max-min rate for different locations of MBS (positions) as depicted on Fig. 5. From the Fig. 5, it is accurately observable that if MBS location alters from (500, 500), (600, 600), (700, 700), (800, 800), and (900, 900), the max-min rate of users decreases for all the schemes. This is because the more the MBS is placed far from the UAV, the more the WB rate reduces which eventually affects the user rate due to the wireless backhaul's flow constraint. In addition to that, our proposed scheme still gives out a better performance compared to the other three scenarios.

Futhermore, we scrutinize how the max-min rate alters when the cell radius varies from 100 to 400 m. From Fig. 6, we notice that the larger the size of cell gets, the less the max-min rate becomes. This is due to the fact that the more the cell radius increases, the more the distance between UAV and N GUs increases, which eventually decreases the channel gain. Thus, the rate of users reduces drastically. Even if the max-min rate reduces for all schemes, our proposed algorithm outperforms the other alternatives.

Finally, to detect how the noise affects our system, we plot the user max-min rate versus various values of noise power density as illustrated on Fig. 7. The increase in noise density obviously lead to a poor user rate. Inspite of that, our proposed scheme still gives better outcomes compared to the remaining alternatives.

V. CONCLUSION

In this paper, we have scrutinized the UAV-enabled WB network in which NOMA is incorporated so as to boost up

the masssive connectivity. More specifically, we have purposed to maximize the minimum GU's achievable rate while optimizing the bandwidth allocation, UAV's power allocation and placement. To ease the complexity of our non-convex problem and to attain the optimal solution as well, we have proposed a path-following algorithm which iterated easily till convergence. In a nutshell, by varying diverse parameters in our simulations, i.e., transmit power and position of MBS, noise density, we have noticed that the wireless backhaul plays a phenomenal impact on the performance of our proposed scheme and the user ground rate as well. In addition to that, we have reckoned that the suggested joint optimization of bandwidth allocation, power allocation and placement for a UAV-enabled wireless backhaul networks; attained a better performance.

REFERENCES

[1] B. Li, Z. Fei, and Y. Zhang, "UAV communications for 5G and beyond: Recent advances and future trends," *IEEE Internet Things J.*, vol. 6, no. 2, pp. 2241–2263, Apr. 2019.

[2] R. Ruby, K. Wu, Q.-V. Pham, and B. M. ElHalawany, "Aiding a disaster spot via an UAV-based mobile AF relay: Joint trajectory and power optimization," in *Proc. 18th ACM Symp. Mobility Manage. Wireless Access*, New York, NY, USA, Nov. 2020, pp. 105–113.

[3] Q. Wu, L. Liu, and R. Zhang, "Fundamental trade-offs in communication and trajectory design for UAV-enabled wireless network," *IEEE Wireless Commun.*, vol. 26, no. 1, pp. 36–44, Feb. 2019.

[4] B. Galkin, J. Kibilda, and L. A. DaSilva, "Backhaul for low-altitude UAVs in urban environments," in *Proc. IEEE Int. Conf. Commun. (ICC)*, Kansas City, MO, USA, May 2018, pp. 1–6.

[5] E. Kalantari, M. Z. Shakir, H. Yanikomeroglu, and A. Yongacoglu, "Backhaul-aware robust 3D drone placement in 5G+ wireless networks," in *Proc. IEEE Int. Conf. Commun. Workshops (ICC Workshops)*, Paris, France, May 2017, pp. 109–114.

[6] C. Qiu, Z. Wei, Z. Feng, and P. Zhang, "Joint resource allocation, placement and user association of multiple UAV-mounted base stations with in-band wireless backhaul," *IEEE Wireless Commun. Lett.*, vol. 8, no. 6, pp. 1575–1578, Dec. 2019.

[7] C. Pan, J. Yi, C. Yin, J. Yu, and X. Li, "Joint 3D UAV placement and resource allocation in software-defined cellular networks with wireless backhaul," *IEEE Access*, vol. 7, pp. 104279–104293, 2019.

[8] M. F. Sohail, C. Y. Leow, and S. Won, "Non-orthogonal multiple access for unmanned aerial vehicle assisted communication," *IEEE Access*, vol. 6, pp. 22716–22727, 2018.

[9] P. K. Sharma and D. I. Kim, "UAV-enabled downlink wireless system with non-orthogonal multiple access," in *Proc. IEEE Globecom Workshops (GC Wkshps)*, Singapore, Dec. 2018, pp. 1–6.

[10] Y. Liu, Z. Qin, Y. Cai, Y. Gao, G. Y. Li, and A. Nallanathan, "UAV communications based on non-orthogonal multiple access," *IEEE Wireless Commun.*, vol. 26, no. 1, pp. 52–57, Feb. 2019.

[11] X. Liu, J. Wang, N. Zhao, Y. Chen, S. Zhang, Z. Ding, and F. R. Yu, "Placement and power allocation for NOMA-UAV networks," *IEEE Wireless Commun. Lett.*, vol. 8, no. 3, pp. 965–968, Jun. 2019.

[12] M. S. Ali, H. Tabassum, and E. Hossain, "Dynamic user clustering and power allocation for uplink and downlink non-orthogonal multiple access (NOMA) systems," *IEEE Access*, vol. 4, pp. 6325–6343, 2016.

[13] W. U. Khan, J. Liu, F. Jameel, V. Sharma, R. Jantti, and Z. Han, "Spectral efficiency optimization for next generation NOMA-enabled IoT networks," *IEEE Trans. Veh. Technol.*, vol. 69, no. 12, pp. 15284–15297, Dec. 2020.

[14] F. Jameel, S. Zeb, W. U. Khan, S. A. Hassan, Z. Chang, and J. Liu, "NOMA-enabled backscatter communications: Toward battery-free IoT networks," *IEEE Internet Things Mag.*, vol. 3, no. 4, pp. 95–101, Dec. 2020.

[15] W. U. Khan, F. Jameel, T. Ristaniemi, S. Khan, G. A. S. Sidhu, and J. Liu, "Joint spectral and energy efficiency optimization for downlink NOMA networks," *IEEE Trans. Cognit. Commun. Netw.*, vol. 6, no. 2, pp. 645–656, Jun. 2020.

[16] Z. H. E. Tan, A. S. Madhukumar, R. P. Sirigina, and A. K. Krishna, "NOMA-aided multi-UAV communications in full-duplex heterogeneous networks," *IEEE Syst. J.*, early access, Aug. 25, 2020, doi: 10.1109/JSYST.2020.3014205.

[17] H. E. Tan Zheng, A. S. Madhukumar, R. P. Sirigina, and A. K. Krishna, "An outage probability analysis of full-duplex NOMA in UAV communications," in *Proc. IEEE Wireless Commun. Netw. Conf. (WCNC)*, Marrakesh, Morocco, Apr. 2019, pp. 1–5.

[18] A. Rahmati, Y. Yapici, N. Rupasinghe, I. Guvenc, H. Dai, and A. Bhuyan, "Energy efficiency of RSMA and NOMA in cellular-connected mmWave UAV networks," in *Proc. IEEE Int. Conf. Commun. Workshops (ICC Workshops)*, Shanghai, China, May 2019, pp. 1–6.

[19] Y. Li, H. Zhang, K. Long, S. Choi, and A. Nallanathan, "Resource allocation for optimizing energy efficiency in NOMA-based fog UAV wireless networks," *IEEE Netw.*, vol. 34, no. 2, pp. 158–163, Mar. 2020.

[20] R. Tang, J. Cheng, and Z. Cao, "Joint placement design, admission control, and power allocation for NOMA-based UAV systems," *IEEE Wireless Commun. Lett.*, vol. 9, no. 3, pp. 385–388, Mar. 2020.

[21] Z. Hadzi-Velkov, S. Pejoski, N. Zlatanov, and R. Schober, "UAV-assisted wireless powered relay networks with cyclical NOMA-TDMA," *IEEE Wireless Commun. Lett.*, vol. 9, no. 12, pp. 2088–2092, Dec. 2020.

[22] R. Zhang, X. Pang, J. Tang, Y. Chen, N. Zhao, and X. Wang, "Joint location and transmit power optimization for NOMA-UAV networks via updating decoding order," *IEEE Wireless Commun. Lett.*, vol. 10, no. 1, pp. 136–140, Jan. 2021.

[23] A. Kilzi, J. Farah, C. A. Nour, and C. Douillard, "Analysis of drone placement strategies for complete interference cancellation in two-cell NOMA CoMP systems," *IEEE Access*, vol. 8, pp. 179055–179069, 2020.

[24] J. Wang, M. Liu, J. Sun, G. Gui, H. Gacanin, H. Sari, and F. Adachi, "Multiple unmanned aerial vehicles deployment and user pairing for non-orthogonal multiple access schemes," *IEEE Internet Things J.*, vol. 8, no. 3, pp. 1883–1895, Feb. 2020.

[25] X. Diao, J. Zheng, Y. Wu, Y. Cai, and A. Anpalagan, "Joint trajectory design, task data, and computing resource allocations for NOMA-based and UAV-assisted mobile edge computing," *IEEE Access*, vol. 7, pp. 117448–117459, 2019.

[26] W. Mei and R. Zhang, "Uplink cooperative NOMA for cellular-connected UAV," *IEEE J. Sel. Topics Signal Process.*, vol. 13, no. 3, pp. 644–656, Jun. 2019.

[27] T. Zhang, Z. Wang, Y. Liu, W. Xu, and A. Nallanathan, "Caching placement and resource allocation for cache-enabling UAV NOMA networks," *IEEE Trans. Veh. Technol.*, vol. 69, no. 11, pp. 12897–12911, Nov. 2020.

[28] K. Sarfo, K. Wang, and K. Ntiamoah-Sarpong, "Estimation of UAV to UAV performance as a hotspot by proposed friss model on downlink AF cooperative NOMA," in *Proc. IEEE 10th Int. Conf. Electron. Inf. Emergency Commun. (ICEIEC)*, Beijing, China, Jul. 2020, pp. 5–9.

[29] Q.-V. Pham, T. Huynh-The, M. Alazab, J. Zhao, and W.-J. Hwang, "Sum-rate maximization for UAV-assisted visible light communications using NOMA: Swarm intelligence meets machine learning," *IEEE Internet Things J.*, vol. 7, no. 10, pp. 10375–10387, Oct. 2020.

[30] S. K. Zaidi, S. F. Hasan, X. Gui, N. Siddique, and S. Ahmad, "Exploiting UAV as NOMA based relay for coverage extension," in *Proc. 2nd Int. Conf. Comput. Appl. Inf. Secur. (ICCAIS)*, May 2019, pp. 1–5.

[31] X. Li, Q. Wang, Y. Liu, T. A. Tsiftsis, Z. Ding, and A. Nallanathan, "UAV-aided multi-way NOMA networks with residual hardware impairments," *IEEE Wireless Commun. Lett.*, vol. 9, no. 9, pp. 1538–1542, Sep. 2020.

[32] X. Jiang, Z. Wu, Z. Yin, Z. Yang, and N. Zhao, "Power consumption minimization of UAV relay in NOMA networks," *IEEE Wireless Commun. Lett.*, vol. 9, no. 5, pp. 666–670, May 2020.

[33] A. A. Nasir, H. D. Tuan, T. Q. Duong, and H. V. Poor, "UAV-enabled communication using NOMA," *IEEE Trans. Commun.*, vol. 67, no. 7, pp. 5126–5138, Jul. 2019.

[34] T. M. Nguyen, W. Ajib, and C. Assi, "A novel cooperative NOMA for designing UAV-assisted wireless backhaul networks," *IEEE J. Sel. Areas Commun.*, vol. 36, no. 11, pp. 2497–2507, Nov. 2018.

[35] P. Li and J. Xu, "UAV-enabled cellular networks with multi-hop backhauls: Placement optimization and wireless resource allocation," in *Proc. IEEE Int. Conf. Commun. Syst. (ICCS)*, Chengdu, China, Dec. 2018, pp. 110–114.

[36] M.-J. Youssef, J. Farah, C. A. Nour, and C. Douillard, "Full-duplex and backhaul-constrained UAV-enabled networks using NOMA," *IEEE Trans. Veh. Technol.*, vol. 69, no. 9, pp. 9667–9681, Sep. 2020.

[37] M. Mozaffari, W. Saad, M. Bennis, Y.-H. Nam, and M. Debbah, "A tutorial on UAVs for wireless networks: Applications, challenges, and open problems," *IEEE Commun. Surveys Tuts.*, vol. 21, no. 3, pp. 2334–2360, 3rd Quart., 2019.
[38] S. M. R. Islam, N. Avazov, O. A. Dobre, and K.-S. Kwak, "Power-domain non-orthogonal multiple access (NOMA) in 5G systems: Potentials and challenges," *IEEE Commun. Surveys Tuts.*, vol. 19, no. 2, pp. 721–742, 2nd Quart., 2017.
[39] Z. Ding, P. Fan, and H. V. Poor, "Impact of user pairing on 5G nonorthogonal multiple-access downlink transmissions," *IEEE Trans. Veh. Technol.*, vol. 65, no. 8, pp. 6010–6023, Aug. 2016.
[40] S. Boyd and L. Vandenberghe, *Convex Optimization*. Cambridge, U.K.: Cambridge Univ. Press, 2004.
[41] Z. Sheng, H. D. Tuan, A. A. Nasir, T. Q. Duong, and H. V. Poor, "Power allocation for energy efficiency and secrecy of wireless interference networks," *IEEE Trans. Wireless Commun.*, vol. 17, no. 6, pp. 3737–3751, Jun. 2018.

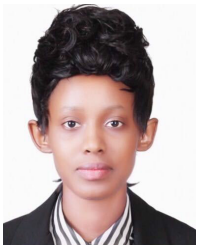

NADIA IRADUKUNDA received the B.S. degree from the College of Science and Technology, University of Rwanda, in 2016, and the M.S. degree in electronic and telecommunication engineering from Inje University, South Korea, in 2019, where she is currently pursuing the Ph.D. degree with the Department of Information and Communication Systems. Her research interests include wireless resource allocation and spectrum management, wireless communications and networking, probability and random process, convex optimization, cognitive radio networks, UAV, and wireless backhaul. She received the Korean Multimedia Systems (KMMS) Best Paper Award, in Fall 2018 and also the 2018 Excellent Academic Achievement Award from the National Institute for International Education (NIIED), Ministry of Education, South Korea.

QUOC-VIET PHAM (Member, IEEE) received the B.S. degree in electronics and telecommunications engineering from Hanoi University of Science and Technology, Vietnam, in 2013, and the Ph.D. degree in telecommunications engineering from Inje University, South Korea, in 2017. He is currently a Research Professor with the Korean Southeast Center for the 4th Industrial Revolution Leader Education, Pusan National University, South Korea. He has been granted the Korea NRF Funding for outstanding young researchers for the term 2019–2023. His research interests include convex optimization, game theory, and machine learning to analyze and optimize edge/cloud computing systems and future wireless systems. He received the Best Ph.D. Dissertation Award in Engineering from Inje University in 2017. He received the top reviewer award from the IEEE Transactions on Vehicular Technology in 2020. He is an Associate Editor of Journal of Network and Computer Applications (Elsevier) and a Review Editor of Frontiers in Communications and Networks.

MING ZENG (Member, IEEE) received the B.E. and master's degrees from the Beijing University of Posts and Telecommunications, China, in 2013 and 2016, respectively, and the Ph.D. degree in telecommunications engineering from Memorial University, Canada, in 2020. He is currently an Assistant Professor with the Department of Electrical Engineering and Computer Engineering, Laval University, Canada. He has published more than 45 articles and conferences in first-tier IEEE journals and proceedings, and his work has been cited over 1150 times per Google Scholar. His research interests include resource allocation for beyond 5G systems, and machine learning empowered optical communications. He serves as an Associate Editor for the IEEE Open Journal of the Communications Society.

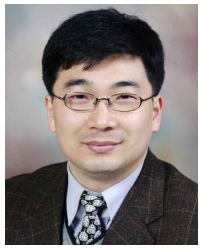

HEE-CHEOL KIM received the B.Sc. degree from the Department of Mathematics, the M.Sc. degree from the Department of Computer Science, Sogang University, South Korea, and the Ph.D. degree in numerical analysis and computing science from Stockholm University, Sweden, in 2001. He is currently a Professor with the Department of Computer Engineering and the Head of the Institute of Digital Anti-aging Healthcare, Inje University, South Korea. He has published more than 100 articles concerning the following areas. His research interests include the areas of artificial intelligence, applied machine learning, human–computer interaction, and social computing.

WON-JOO HWANG (Senior Member, IEEE) received the B.S. and M.S. degrees in computer engineering from Pusan National University, Busan, South Korea, in 1998 and 2000, respectively, and the Ph.D. degree in information systems engineering from Osaka University, Osaka, Japan, in 2002. From 2012 to 2019, he was a Full Professor with Inje University, Gimhae, South Korea. Since January 2020, he has been a Full Professor with the School of Biomedical Convergence Engineering, Pusan National University, Yangsan, South Korea. His research interests include network optimization and cross layer design.